BIOCHEMISTRY

 Volume 45, Number 11 March 21, 2006

Accelerated Publications

Hydration of the Folding Transition State Ensemble of a Protein†

Ludovic Brun,‡ Daniel G. Isom,§ Priya Velu,§ Bertrand García-Moreno,§ and Catherine Ann Royer*,‡

INSERM U554, Montpellier, F-34090 France, Université Montpellier I, CNRS, UMR 5048, and Department of Biophysics, Johns Hopkins University, Baltimore, Maryland 21218

Received December 26, 2005; Revised Manuscript Received February 9, 2006

ABSTRACT: A complete description of the mechanisms of protein folding requires knowledge of the structural and physical character of the folding transition state ensembles (TSEs). A key question concerning the role of hydration of the hydrophobic core in determining folding mechanisms remains. To address this, we probed the state of hydration of the TSE of staphylococcal nuclease (SNase) by examining the fluorescence-detected pressure-jump relaxation behavior of six SNase variants in which a residue in the hydrophobic core, Val-66, was replaced with polar or ionizable residues (Lys, Arg, His, Asp, Glu, and Asn). Because of a large positive activation volume for folding, the major effect of pressure on the wild-type protein is to decrease the folding rate. By the time wild-type SNase reaches the folding transition state, most water has already been expelled from its hydrophobic core. In contrast, the major effect of pressure on the variant proteins is an increase in the unfolding rate due to a large negative activation volume for unfolding. This results from a significant increase in the level of hydration of the TSE when an internal ionizable group is present. These data confirm that the role of water in the folding reaction can differ from protein to protein and that even a single substitution in a critical position can modulate significantly the properties of the TSE.

The exponential nature of protein folding kinetics suggests the existence of rate-limiting energy barriers between the folded and unfolded states. The lack of a detailed understanding of this barrier and of the attendant rate-limiting ensemble of states still limits our ability to describe mechanisms of folding in detail. Although use of ϕ value analysis (*1*−*4*) to describe the character of the folding transition state ensembles (TSEs)[1] remains controversial (*5*, *6*), a self-consistent view is emerging (*7*−*12*). Considerable differences in the TSEs of different proteins have been observed (*13*, *14*), but in general, nativelike structures are thought to dominate the TSE, possibly even with many side chains already fully dehydrated but with few of them satisfying their native contacts (*5*, *6*, *15*).

Computational analyses of ϕ values have significantly influenced the prevailing views on the structural character of the TSE (*16*−*28*), which is thought to be determined primarily by the topology of the protein and not by detailed energetic factors (*17*, *24*, *29*, *30*). Some computational studies suggest that TSEs consist mostly of expanded and distorted native structure. In MD-based studies, subsets of nucleating interactions are assigned key roles (*19*, *21*, *22*, *27*), but this is not fully consistent with experimental data (*5*, *6*, *31*).

Despite this progress in characterizing the TSE, the central question of the role of hydration in determining folding rates and mechanisms remains unanswered. Computational studies

† This work was supported by the National Institutes of Health (Grant R01-GM61597 to B.G.-M.) and by INSERM and the COST Program (C.R.), as well as undergraduate research support from JHU to B.G.-M.

* To whom correspondence should be addressed. Phone: 33 4 67 41 79 02. Fax: 33 4 67 41 79 13. E-mail: royer@cbs.cnrs.fr.

‡ INSERM U554.

§ Johns Hopkins University.

[1] Abbreviations: SNase, staphylococcal nuclease; TSE, transition state ensemble.

10.1021/bi052638z CCC: $33.50
Published on Web 02/24/2006

Table 1: Volume Changes for the Folding−Unfolding Transitions of SNase Cavity Mutants[a]

	WT SNase at pH 6	WT Δ+PHS at pH 5 and 2 M GuHCl	Δ+PHS V66K at pH 6	Δ+PHS V66R at pH 6	Δ+PHS V66D at pH 8	Δ+PHS V66E at pH 8 and 1 M GuHCl	Δ+PHS V66H at pH 8 and 1 M GuHCl	Δ+PHS V66N at pH 5 and 1 M GuHCl
$\Delta V_f°$ (mL/mol)	64 ± 5	41 ± 4	60 ± 6	67 ± 5	62 ± 7	84 ± 10	94.0 ± 8	99 ± 14
$\Delta V_f^‡$ (mL/mol)	56 ± 3	nd[b]	15	14.6	9.5	30	52	46
$\Delta V_u^‡$ (mL/mol)	−8	nd[b]	−45 ± 3	−52 ± 4	−53 ± 4	−54 ± 8	−42 ± 8	−53 ± 9
$\Delta G_f°$ (kcal/mol)	−3.6 ± 0.3	−2.3 ± 2	−3.0 ± 0.3	−1.9 ± 0.2	−4.4 ± 0.4	−1.8 ± 0.3	−5.1 ± 0.4	−4.0 ± 0.6
$k_f°$ (s^{-1})	0.28 ± 0.09	nd[b]	0.03	0.06	0.01	4×10^{-4}	0.01	0.002
$k_u°$ (s^{-1})	6×10^{-4}	nd[b]	$(1.9 \pm 0.6) \times 10^{-4}$	$(2.3 \pm 0.5) \times 10^{-3}$	$(2.6 \pm 1.3) \times 10^{-6}$	$(1.9 \pm 0.8) \times 10^{-5}$	$(1.7 \pm 1.5) \times 10^{-6}$	$(1.9 \pm 1.3) \times 10^{-6}$

[a] At pH <7, the buffer was 50 mM bis-Tris, and at pH >7, the buffer was 50 mM Tris. [b] Not determined.

suggest that the conformations populated in the TSE consist mostly of native structure with a highly solvated hydrophobic core. The final step in the folding reaction is thought to involve packing of the hydrophobic core and concomitant, cooperative squeezing of water out of the core (*16*, *20*, *25*, *32*). Water in the core of the TSE could prevent nonnative contacts from being formed (*28*). Experimentally, it has been shown that replacement of a hydrophobic core side chain with an isosteric polar one can alter the hydration of the TSE when residues crucial to the folding mechanism are targeted (*32*). These experimental findings can be modeled using a desolvation potential (*16*). They support the view of the TSE as a highly hydrated state.

The emerging view of TSEs as a highly hydrated, nativelike state is not consistent with previous results from pressure-jump relaxation studies of wild-type (WT) staphylococcal nuclease (SNase) (*33*). These studies revealed that the rate-limiting step in folding was accompanied by significant dehydration and that the TSE for this protein was relatively dry. Indeed, pressure perturbation offers a unique experimental means for probing the role of hydration changes in protein conformational changes (*34*) because pressure effects arise from differences in the specific volumes of the various (folded, intermediates, unfolded, transition) states of the protein. These differences in specific volume are linked directly to the degree and type (polar or nonpolar) of hydration and to the existence or loss of cavity volume (*35*, *36*), which also involve hydration and dehydration, respectively. Most proteins studied to date exhibit a larger specific volume in the folded state than in the unfolded state; hence, the application of pressure leads to their unfolding. Our earlier pressure-jump relaxation studies demonstrated that the effect of pressure on the stability of WT SNase arises primarily from a pressure-induced decrease in the folding rate constant due to a positive activation volume for this reaction, suggesting significant dehydration of the transition state ensemble (*33*). Similar pressure-jump relaxation studies of the folding of six other proteins indicated that significant (although less) dehydration accompanied the rate-limiting step in folding of these proteins as well (*37*−*42*).

To probe the state of hydration of the TSE of SNase in depth, we performed pressure unfolding experiments with variants in which a deeply buried hydrophobic residue, Val-66, was replaced with Arg, Lys, His, Asp, Glu, or Asn. Charged and polar groups are well hydrated in water; therefore, removal of these groups from water for placement into the core of the protein is energetically unfavorable. The introduction of ionizable and polar groups into the protein interior was expected to perturb the TSE of the protein and to allow clarification of the role of water in the final stages of folding with an unprecedented level of detail.

METHODS

Replacement of core hydrophobic residues with polar or ionizable residues is energetically disfavored (*43*−*50*). For this reason, the variants with the internal Val-66 residue substituted with Arg, Lys, His, Asp, Glu, or Asn were engineered using a hyperstable form of SNase known as Δ+PHS after the set of substitutions (P117G, H124L, S128A, G50F, and V51N) and deletions (Δ44−49). WT SNase and all of the Δ+PHS proteins were produced and purified as described previously (*51*). The pressure-jump experiments were carried out in either Tris or bis-Tris buffer (Aldrich) at 50 mM and at the pH indicated in Table 1 to avoid pressure-induced changes in the pH (*52*). GuHCl (Aldrich) was dissolved in the appropriate buffer, the pH adjusted, and the solution used at the concentration given in Table 1. The protein concentration was near 70 μM.

High-pressure experiments were carried out using a stainless steel high-pressure cell designed in our laboratory and fitted with sapphire windows. The high-pressure-generating equipment has been described previously (*53*). High-purity (18 MΩ) water was used as the pressure-generating liquid. Fluorescence measurements were made using the detection from an ISS KOALA instrument (ISS, Champaign, IL) and an ISS excitation source and monochromator coupled to the high-pressure cell via an optical fiber. The excitation and emission monochromator slits were 8 nm, and the excitation wavelength was 295 nm. The emission was set at 335 nm. Emission spectra (310−450 nm) were also acquired once the sample had equilibrated. The acquisition time base was 1 s. Pressure jumps were performed by pumping the pressure with the valve to the high-pressure cell closed, followed by rapid opening of the valve. Solution conditions were adjusted with pH or guanidine hydrochloride to decrease the stability of the proteins so that pressures below 4 kbar (400 MPa) were sufficient to unfold the variants that were tested. We have shown previously that changes in pH or in the concentration of GuHCl change the stability of SNase without affecting the volume change measured by pressure unfolding (*53*, *54*).

Equilibrium unfolding profiles were analyzed for the volume change (ΔV_f) and free energy of folding (ΔG_f) using the analysis program Bioeqs and an analytical rather than numerical model of two-state folding.

$$\frac{d\Delta G_f}{dp} = -\Delta V_f \quad (1)$$

$$\Delta G_f = -RT \ln K_f \quad (2)$$

$$K_f = \frac{[F]}{[U]} = \frac{I_p - I_i}{I_i - I_p} \quad (3)$$

Uncertainties in the recovered free energy and volume change values were determined by rigorous confidence limit testing and take into account correlations between the fitted parameter.

The pressure-jump relaxation profiles at each pressure were analyzed according to classical transition state theory for a single-exponential decay:

$$I_t = I_o e^{-t/\tau_p} + C \quad (4)$$

For a simple two-state reaction, the relaxation time τ at each pressure is the inverse sum of the folding and unfolding rate constants, $k_{f(p)}$ and $k_{u(p)}$, respectively, at that pressure.

$$\ln \tau_{(p)} = 1/[k_{f(p)} + k_{u(p)}] \quad (5)$$

These rate constants are exponentially dependent upon pressure and the activation volumes for the reactions.

$$k_{f(p)} = k_{fo} e^{-p\Delta V_f^{\ddagger}/RT} \text{ and } k_{u(p)} = k_{uo} e^{-p\Delta V_u^{\ddagger}/RT} \quad (6)$$

Thus, the plots of ln τ versus p are fit using nonlinear least-squares analysis for the values of the activation volumes ($\Delta V_f^{\ddagger}$ and $\Delta V_u^{\ddagger}$) and rate constants (k_{fo} and k_{uo}) for folding and unfolding at atmospheric pressure. We have constrained the analysis to only two parameters, those for either folding (WT) or unfolding (variants), using the equilibrium volume change and free energy for folding according to

$$\Delta G_f^{\circ} = -RT \ln K_f = -RT \ln\left(\frac{k_f}{k_u}\right) \quad (7)$$

such that

$$k_f = k_u K_f \text{ or } k_u = \frac{K_f}{k_f} \quad (8)$$

and

$$\Delta V_f^{\circ} = \Delta V_f^{\ddagger} - \Delta V_u^{\ddagger} \quad (9)$$

such that

$$\Delta V_f^{\ddagger} = \Delta V_f^{\circ} + \Delta V_u^{\ddagger} \text{ or } \Delta V_u^{\ddagger} = \Delta V_f^{\ddagger} - \Delta V_f^{\circ} \quad (10)$$

Uncertainties reported are calculated from the diagonal of the correlation matrix and correspond to 95% confidence limits.

RESULTS AND DISCUSSION

Proteins with Internal Polar or Ionizable Residues. Fluorescence-detected pressure-jump relaxation experiments were performed with V66K, V66R, V66H, V66D, V66E, and V66H variants of the Δ+PHS hyperstable nuclease. Crystal structures of all but the His-66 variant have been determined previously under room-temperature and cryogenic conditions (Figure 1) (*45*, *47*, *48*, *50*, *55*). With the exception of the V66R variant, in which the β-barrel releases a strand to expose Arg-66 to water (D. A. Karp, A. G. Gittis, and B. García-Moreno, manuscript in preparation), under conditions near neutral pH, where the internal ionizable groups are neutral, the residues at position 66 are indeed buried in the core of the protein in a hydrophobic pocket. Under these conditions, there are also no detectable differences between the native states of the variant proteins and of the background protein. One or two internal water molecules have been observed hydrating the internal polar moieties in cryogenic structures with internal Asp, Glu, Asn, Gln, Tyr, and Trp at position 66. Molecular dynamics simulations also suggest that two or three water molecules can penetrate into the hydrophobic core of WT SNase at room temperature and pressure, even in the absence of internal polar or ionizable groups (*56*). Internal water molecules have never been observed crystallographically in the WT protein.

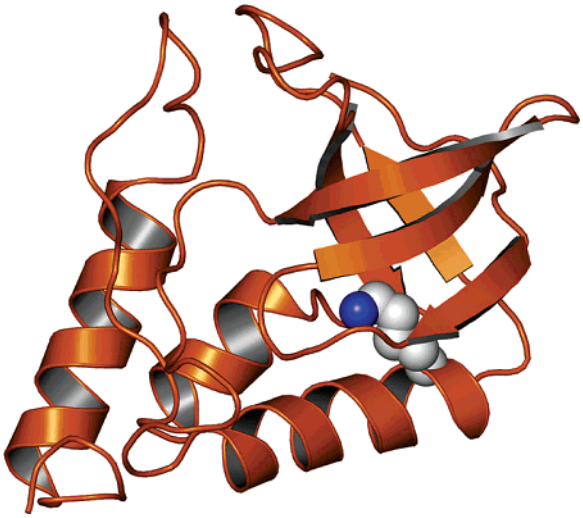

FIGURE 1: Schematic of the structure of the SNase V66K variant with K66 in a space-filling representation (*50*).

The pK_a values of the internal ionizable groups have been measured previously: 5.7 for Lys-66 (*46*−*48*), 8.9 for Asp-66 (*48*), 9.2 for Glu-66 (*45*), <4 for His-66, and >10 for Arg-66 (D. A. Karp, A. G. Gittis, and García-Moreno, manuscript in preparation). These pK_a values are shifted substantially relative to the pK_a values of ionizable groups in water. This effect is driven largely by the dehydration of the ionizable groups when they are in internal positions in the protein (*46*).

Equilibrium Unfolding by Pressure. The fluorescence-detected pressure-induced unfolding profiles of wild-type and variant SNase (Figure 2) were fit to a two-state unfolding model. The values for the volume change and free energy for folding at atmospheric pressure (ΔV_f° and ΔG_f°) recovered from this analysis are listed in Table 1. The ΔV_f° for wild-type SNase is within error of our previously reported measurement of 70 ± 10 mL/mol (at 21 °C rather than 23 °C) (*33*, *57*). The volume change for folding the Δ+PHS was 41 mL/mol, significantly smaller than that of the wild type. The substitutions and deletions used to create the Δ+PHS hyperstable form of SNase are at external sites and produce only local changes in the structure (*43*, *44*). We have also shown previously that the P117G/H124L double substitution has no effect on the volume change of unfolding (*54*). The other mutations and deletions in Δ+PHS are unlikely to result in significant structural changes since they are all exposed. Hence, the difference in overall volume change between Δ+PHS and WT SNase must arise from stabilization of residual structure in the unfolded state in the Δ+PHS variant. Clearly, introduction of ionizable residues

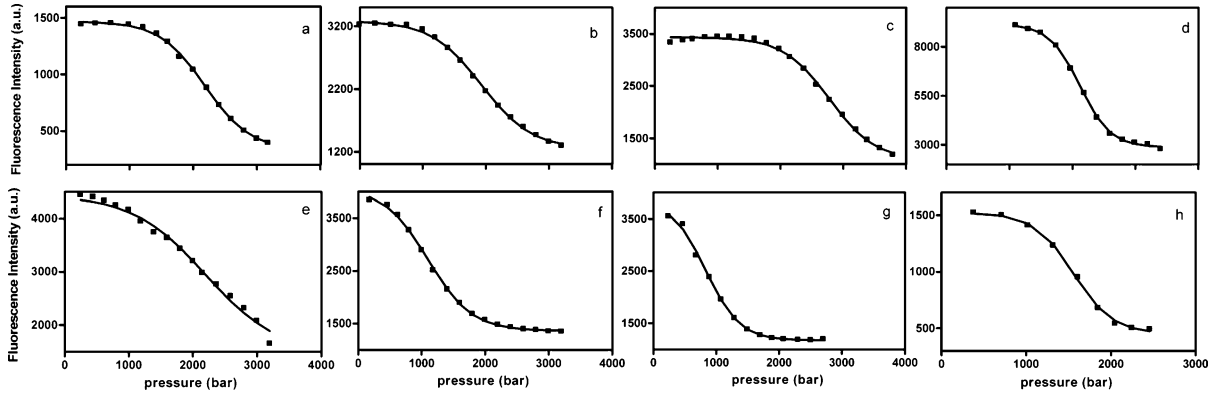

FIGURE 2: Equilibrium fluorescence-detected high-pressure unfolding profiles for SNase and its variants: (a) WT SNase, (b) Δ+PHS V66K, (c) Δ+PHS V66D, (d) Δ+PHS V66H, (e) Δ+PHS, (f) Δ+PHS V66R, (g) Δ+PHS V66E, and (h) Δ+PHS V66N. Conditions are given in Table 1. The temperature was 23 °C. Lines through the points represent fits of the data to eq 1 as described in the text.

in the hydrophobic core disrupts this residual structure in the unfolded state, rendering the overall volume change upon unfolding comparable to that of the WT SNase.

With the exception of Arg-66, the other internal ionizable groups were largely neutral under the conditions that were tested (*45*, *46*, *48*). We expected a contribution to the pressure effects from the electrostriction related to the ionization of these internal ionizable residues upon unfolding. This should have led to an increase the magnitude of the $\Delta V_f°$ above that of the background Δ+PHS protein. While the variants with V66K, V66E, and V66D all exhibited $\Delta V_f°$ values greater than that for the Δ+PHS background protein, consistent with electrostriction, those with V66R, V66H, and V66N substitutions unfold with $\Delta V_f°$ values that are as large or even larger than those for the proteins in which electrostriction was anticipated, yet in these variants, electrostriction cannot be a factor because these groups are either neutral (His, Asn) or charged (Arg) in both folded and unfolded states at the pH where the experiments are performed. Although we have shown previously that an increase in the size of the small internal cavity around position 66 will result in larger $\Delta V_f°$ values (*35*), this also cannot be the reason behind the larger $\Delta V_f°$ values measured for the variants with internal polar and ionizable side chains because these side chains would actually decrease the volume of the small internal cavity. Instead, the large $\Delta V_f°$ must reflect the destabilization of residual structure in the unfolded state. We note that the free energy values cannot be compared among variants since the conditions of the experiments were chosen to tune the pressure-induced unfolding into the appropriate range for our apparatus. However, the free energy measured by pressure and chemical denaturation for all variants are in agreement (data for chemical denaturation not shown), corroborating the validity of the thermodynamic parameters obtained by pressure unfolding.

Pressure-Jump Relaxation Kinetics. Pressure-jump relaxation profiles at multiple pressures were obtained for all the variants. The Δ+PHS protein was not studied because the relaxation was faster than the 2 s dead time of our instrument. This very fast relaxation time is consistent with a large increase in the folding rate for this hyperstable variant. All of the other variants exhibited single-exponential relaxation curves, indicative of simple two-state kinetic behavior, as shown previously for WT SNase at high pressures under a variety of conditions (*33*, *57*). This loss of kinetic complexity

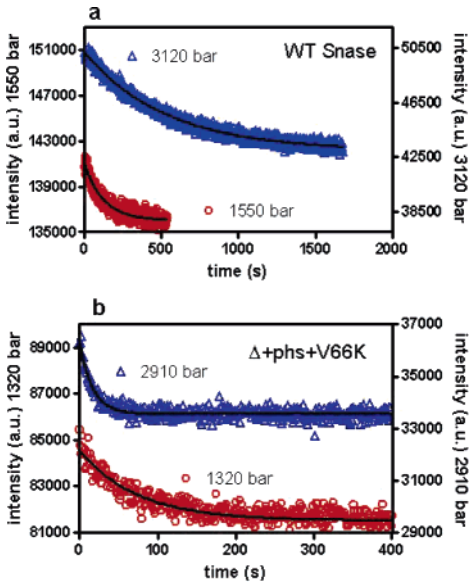

FIGURE 3: Pressure-jump fluorescence-detected relaxation profiles. (a) For WT SNase, the circles correspond to the intensity relaxation after a jump from 1350 to 1550 bar whereas the triangles correspond to the relaxation after a jump from 2920 to 3120 bar. (b) For the Δ+PHS V66K variant, the circles correspond to the intensity relaxation after a jump from 1100 to 1320 bar whereas the triangles correspond to the relaxation after a jump from 2710 to 2920 bar. The data were fit to a single-exponential decay model (eq 4), and the lines drawn through the points correspond to the fits. Conditions are those described in the legend of Figure 2. The data illustrate that for the wild type, relaxation slows significantly as the pressure is increased, whereas for the Δ+PHS V66K variant, increasing pressure leads to much faster relaxation.

at high pressure appears to arise from the pressure inhibition of proline isomerization (*54*, *58*).

For WT SNase (Figure 3a), the relaxation times increase significantly with an increase in pressure, as previously reported (*33*, *57*). Strikingly, the V66K, V66R, V66D, and V66E variants of Δ+PHS exhibited the opposite behavior (shown in Figure 3b for the Δ+PHS/V66K variant). As the pressure was increased, the relaxation times became significantly shorter. The relaxation profiles at each pressure for each variant were analyzed for a single-exponential relaxation time. Plots of the natural logarithm of these relaxation times (ln τ vs pressure) are shown in Figure 4 for WT SNase and for the V66N, V66K, V66R, V66D, and V66E variants of

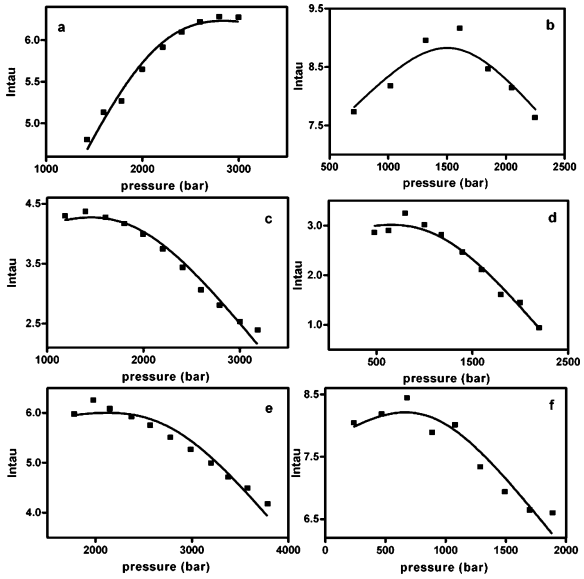

FIGURE 4: Dependence of the natural logarithm of the relaxation time on the final pressure. The values for the relaxation times are those obtained from the fits of data like those in Figure 3. The lines through the points represent fits of the data according to eq 5, as described in the text: (a) WT SNase, (b) Δ+PHS V66N, (c) Δ+PHS V66K, (d) Δ+PHS V66R, (e) Δ+PHS V66D, and (f) Δ+PHS V66E.

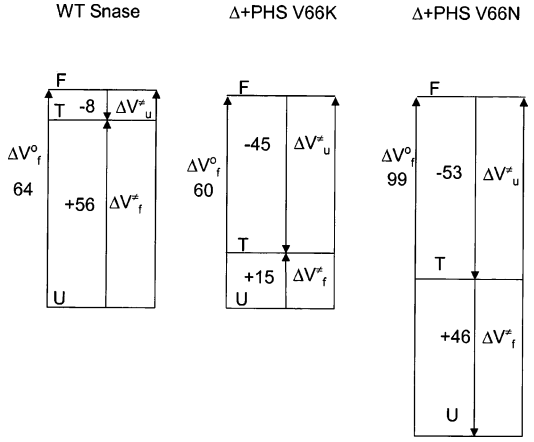

FIGURE 5: Volume diagrams for the folding−unfolding reactions of WT SNase and two of the variants, Δ+PHS V66K and Δ+PHS V66N. The values for the activation volumes were obtained from the fits of data like those in Figure 4 and the equilibrium unfolding volume. All values were normalized to the same volume for the folded state, based on the fact that the structures of these proteins are nearly identical.

Δ+PHS. The ln τ versus pressure plots for all of the variants were analyzed according to eqs 5 and 6 for the activation volumes and rate constants for either folding or unfolding.

The analysis for the WT protein yielded, as previously reported, a large activation volume for folding and a very small negative activation volume for unfolding (Table 1). In contrast, for the V66K, V66R, V66D, and V66E variants, the activation volume for folding was much smaller than for the wild-type protein, while that for unfolding was very large and negative (Figure 4 and Table 2).

The differences in folding mechanisms of wild-type and variant proteins are described schematically by the volume diagrams in Figure 5. The activation volumes for folding and unfolding combine to yield the overall equilibrium volume changes. The equilibrium unfolding volume changes are somewhat different among the variants tested here. Because the structures of the native state are comparable for the proteins that were studied, the differences in equilibrium volume change must be linked to differences in the degree of hydration of the unfolded state. In the case of the wild-type protein, the volume of the TSE lies near that of the folded state. This is consistent with our prior interpretation that the TSE of WT SNase is highly dehydrated (*33*, *57*). In contrast, the V66K variant exhibits a TSE whose volume is much closer to that of the unfolded state and thus much more hydrated that the WT TSE. For V66N and V66E, the equilibrium unfolding volume change is larger than for the other variants. Since there are no significant structural differences among the native states of these proteins, this is also more likely to reflect an increased level of hydration of the unfolded state. Also, since the folded states of the Δ+PHS background variant and the WT SNase are structurally equivalent and the Δ+PHS mutant is significantly more stable than the WT, it is highly unlikely that these background-stabilizing mutations are responsible for the more open, hydrated transition state observed in the variants of Δ+PHS bearing ionizable residues in their hydrophobic core.

The analysis of the pressure-jump relaxation data presented above is grounded on classical transition state theory. The kinetic and energetic basis of pressure-induced protein unfolding has also been analyzed previously (*59*) with energy landscape theory of protein folding (*60*), using a square well potential that includes a desolvation barrier (*61*, *62*). In this theoretical treatment of a model β-barrel protein, increasing pressure was found to actually lower the transition barrier. Nevertheless, the overall result of pressure was to decrease the folding rate because of a large effect of pressure on the reconfigurational diffusion coefficient, D_Q. This pressure-induced decrease in D_Q suggests that in these simulations, the increase in the rate of folding with an increase in pressure was surpassed by the increase in the roughness of the landscape with an increase in pressure. We have evidence from iso-energetic pressure studies of WT SNase at varying concentrations of stabilizers and denaturants (*57*; Frye, Niemeyer, Royer, Garcia, and Onuchic, unpublished data) that pressure may indeed diminish the pre-exponential factor by a factor of 1.7 kbar^{-1}. However, the overall decrease in the folding rate, over 1 kbar, represents a factor of 7 (Figure 4), demonstrating that pressure indeed increases the free energy at the folding barrier for this protein. The contribution of the pre-exponential factor is, at most, ~25% of the total effect of pressure in this system. In the case of the variants with internal ionizable residues, pressure leads to an increase in the relaxation rate, rather than a slowing of it. A general effect of pressure on the roughness of the folding landscape cannot be invoked to explain our observations. Indeed, pressure may also decrease the D_Q in the case of the variants studied here, but this effect, if it exists, is compensated by a pressure-induced increase in the unfolding rate constant linked to a large, negative activation volume for unfolding.

CONCLUSIONS

The pressure-jump relaxation experiments have revealed a striking and unique difference in the folding mechanisms

of wild-type SN and of variants with internal polar or ionizable groups. Consider as a representative example the case of the V66K variant. The structure of the V66K variant of SNase is essentially identical to the structure of the wild-type protein (*47*, *50*). Under the conditions in which pressure unfolding was performed, the stability of the V66K protein and that of its parent protein are quite similar, and the rate constants for folding and unfolding differ by factors of only 10 and 3, respectively. Even the equilibrium pressure unfolding profiles of the two proteins are almost indistinguishable. Yet the pressure dependence of their folding kinetics suggests that these two proteins fold via very different mechanisms.

The differences in the state of hydration of the TSE in the variants and in the wild-type protein can be rationalized in terms of the high unfavorable free energy that would be required to neutralize and dehydrate a charged side chain if it were to be buried in a nativelike TSE. Internal polar and ionizable groups would promote a hydrated TSE in which the polar and ionizable group destined to occupy internal positions in the native state can remain charged and fully solvated. The pressure unfolding data of the variants with internal polar or ionizable groups are very significant because they reinforce the view that the TSE of wild-type SNase is highly dehydrated.

In many computational studies, based primarily on Go models and desolvation potentials, the native structure is achieved before water is expelled from the hydrophobic core (*16*, *20*, *25*, *28*, *32*). This would appear to be inconsistent with our observations of a highly dehydrated TSE for WT SNase. It is important to note that not all proteins behave the same way. Wild-type SNase (*33*) and CspB (*38*), for example, appear to have highly dehydrated TSEs. The other five proteins that have been examined by pressure unfolding [*trp* repressor (*37*), $P13^{MTCP1}$ (*39*), CI2 (*40*), Tendamistat (*41*), and P23 (*42*)] exhibit specific volumes for their TSEs that lie one-half to three-fourths of the way between those of the unfolded and folded states. This is consistent with the TSEs of these proteins having lost water relative to the unfolded state, but nonetheless remaining significantly hydrated. Indeed, in replica exchange MD simulations of the folding of protein A (*61*), ~25% of the hydrating waters remain at the TSE and are expelled in the final step in folding. This amount of water remaining in the core at the TSE is actually in quite good agreement with the results of the pressure relaxation studies, in which 50−75% of the water is expelled at the TSE, leaving ~25−50% behind. Wild-type SNase appears to be something of an exception (perhaps due to the important size of its hydrophobic core compared to most of the other proteins studied by pressure-jump techniques); its TSE appears to be much closer to that of the native state than is observed in other proteins. We note as well that the activation and equilibrium volume changes calculated from the pressure effects on folding are indicative of the overall (thermodynamic) degree of hydration and are not a quantitative measure of the number of water molecules such that a direct comparison between the simulations and the experiments is not yet possible, particularly since they were not performed on the same protein systems.

These results demonstrate that substitution of a single amino acid can drastically alter the state of hydration of the TSE. The role of hydration in determining the folding mechanism is likely to be highly sequence dependent and influenced by the presence of uncompensated polarity in the protein interior. These data also illustrate the high plasticity of the TSE, which apparently adapts structurally to an energetically costly change in sequence. In the case of wild-type SNase, the folding TSE is already quite dehydrated; thus, the last step in folding does not involve major dehydration of the hydrophobic core. Instead, it might involve the establishment of the native contacts necessary to stabilize side chains in their nativelike conformations in an already dehydrated core (*5*, *6*, *15*, *31*).

REFERENCES

1. Grantcharova, V. P., Riddle, D. S., Santiago, J. V., and Baker, D. (1998) Important role of hydrogen bonds in the structurally polarized transition state for folding of the src SH3 domain, *Nat. Struct. Biol. 5*, 714−720.
2. Grantcharova, V. P., Riddle, D. S., and Baker, D. (2000) Long-range order in the src SH3 folding transition state, *Proc. Natl. Acad. Sci. U.S.A. 97*, 7084−7089.
3. Otzen, D. E., Itzhaki, L. S., elMasry, N. F., Jackson, S. E., and Fersht, A. R. (1994) Structure of the transition state for the folding/unfolding of the barley chymotrypsin inhibitor 2 and its implications for mechanisms of protein folding, *Proc. Natl. Acad. Sci. U.S.A. 91*, 10422−10425.
4. Serrano, L., Matouschek, A., and Fersht, A. R. (1992) The folding of an enzyme. III. Structure of the transition state for unfolding of barnase analysed by a protein engineering procedure, *J. Mol. Biol. 224*, 805−818.
5. Raleigh, D. P., and Plaxco, K. W. (2005) The protein folding transition state: What are ϕ-values really telling us? *Protein Pept. Lett. 12*, 117−122.
6. Sanchez, I. E., and Kiefhaber, T. (2003) Origin of unusual ϕ-values in protein folding: Evidence against specific nucleation sites, *J. Mol. Biol. 334*, 1077−1085.
7. Grantcharova, V. P., and Baker, D. (2001) Circularization changes the folding transition state of the src SH3 domain, *J. Mol. Biol. 306*, 555−563.
8. Lindberg, M., Tangrot, J., and Oliveberg, M. (2002) Complete change of the protein folding transition state upon circular permutation, *Nat. Struct. Biol. 9*, 818−822.
9. Otzen, D. E., Kristensen, O., Proctor, M., and Oliveberg, M. (1999) Structural changes in the transition state of protein folding: Alternative interpretations of curved chevron plots, *Biochemistry 38*, 6499−6511.
10. Otzen, D. E., and Oliveberg, M. (2004) Correspondence between anomalous m- and ΔCp-values in protein folding, *Protein Sci. 13*, 3253−3263.
11. Viguera, A. R., Serrano, L., and Wilmanns, M. (1996) Different folding transition states may result in the same native structure, *Nat. Struct. Biol. 3*, 874−880.
12. Gruebele, M. (2002) Protein folding: The free energy surface, *Curr. Opin. Struct. Biol. 12*, 161−168.
13. Itzhaki, L. S., Otzen, D. E., and Fersht, A. R. (1995) The structure of the transition state for folding of chymotrypsin inhibitor 2 analysed by protein engineering methods: Evidence for a nucleation-condensation mechanism for protein folding, *J. Mol. Biol. 254*, 260−288.
14. Shen, T., Hofmann, C. P., Oliveberg, M., and Wolynes, P. G. (2005) Scanning malleable transition state ensembles: Comparing theory and experiment for folding protein U1A, *Biochemistry 44*, 6433−6439.
15. Frieden, C. (2003) The kinetics of side chain stabilization during protein folding, *Biochemistry 42*, 12439−12446.
16. Cheung, M. S., Garcia, A. E., and Onuchic, J. N. (2002) Protein folding mediated by solvation: Water expulsion and formation of the hydrophobic core occur after the structural collapse, *Proc. Natl. Acad. Sci. U.S.A. 99*, 685−690.
17. Clementi, C., Nymeyer, H., and Onuchic, J. N. (2000) Topological and energetic factors: What determines the structural details of

the transition state ensemble and "en-route" intermediates for protein folding? An investigation for small globular proteins, *J. Mol. Biol. 298*, 937−953.
18. Ding, F., Dokholyan, N. V., Buldyrev, S. V., Stanley, H. E., and Shakhnovich, E. I. (2002) Direct molecular dynamics observation of protein folding transition state ensemble, *Biophys. J. 83*, 3525−3532.
19. Gsponer, J., and Caflisch, A. (2002) Molecular dynamics simulations of protein folding from the transition state, *Proc. Natl. Acad. Sci. U.S.A. 99*, 6719−6724.
20. Guo, W., Lampoudi, S., and Shea, J. E. (2003) Posttransition state desolvation of the hydrophobic core of the src-SH3 protein domain, *Biophys. J. 85*, 61−69.
21. Lindorff-Larsen, K., Vendruscolo, M., Paci, E., and Dobson, C. M. (2004) Transition states for protein folding have native topologies despite high structural variability, *Nat. Struct. Mol. Biol. 11*, 443−449.
22. Lindorff-Larsen, K., Rogen, P., Paci, E., Vendruscolo, M., and Dobson, C. M. (2005) Protein folding and the organization of the protein topology universe, *Trends Biochem. Sci. 30*, 13−19.
23. Onuchic, J. N., Socci, N. D., Luthey-Schulten, Z., and Wolynes, P. G. (1996) Protein folding funnels: The nature of the transition state ensemble, *Folding Des. 1*, 441−450.
24. Shea, J. E., Onuchic, J. N., and Brooks, C. L., III (1999) Exploring the origins of topological frustration: Design of a minimally frustrated model of fragment B of protein A, *Proc. Natl. Acad. Sci. U.S.A. 96*, 12512−12517.
25. Sheinerman, F. B., and Brooks, C. L., III (1998) Calculations on folding of segment B1 of streptococcal protein G, *J. Mol. Biol. 278*, 439−456.
26. Shoemaker, B. A., Wang, J., and Wolynes, P. G. (1999) Exploring structures in protein folding funnels with free energy functionals: The transition state ensemble, *J. Mol. Biol. 287*, 675−694.
27. Vendruscolo, M., Paci, E., Dobson, C. M., and Karplus, M. (2001) Three key residues form a critical contact network in a protein folding transition state, *Nature 409*, 641−645.
28. Wu, X., and Brooks, B. R. (2004) β-Hairpin folding mechanism of a nine-residue peptide revealed from molecular dynamics simulations in explicit water, *Biophys. J. 86*, 1946−1958.
29. Scalley-Kim, M., and Baker, D. (2004) Characterization of the folding energy landscapes of computer generated proteins suggests high folding free energy barriers and cooperativity may be consequences of natural selection, *J. Mol. Biol. 338*, 573−583.
30. Yi, Q., Rajagopal, P., Klevit, R. E., and Baker, D. (2003) Structural and kinetic characterization of the simplified SH3 domain FP1, *Protein Sci. 12*, 776−783.
31. Sanchez, I. E., and Kiefhaber, T. (2003) Evidence for sequential barriers and obligatory intermediates in apparent two-state protein folding, *J. Mol. Biol. 325*, 367−376.
32. Fernandez-Escamilla, A. M., Cheung, M. S., Vega, M. C., Wilmanns, M., Onuchic, J. N., and Serrano, L. (2004) Solvation in protein folding analysis: Combination of theoretical and experimental approaches, *Proc. Natl. Acad. Sci. U.S.A. 101*, 2834−2839.
33. Vidugiris, G. J., Markley, J. L., and Royer, C. A. (1995) Evidence for a molten globule-like transition state in protein folding from determination of activation volumes, *Biochemistry 34*, 4909−4912.
34. Royer, C. A. (2002) Revisiting volume changes in pressure-induced protein unfolding, *Biochim. Biophys. Acta 1595*, 201−209.
35. Frye, K. J., Perman, C. S., and Royer, C. A. (1996) Testing the correlation between ΔA and ΔV of protein unfolding using *m* value mutants of staphylococcal nuclease, *Biochemistry 35*, 10234−10239.
36. Frye, K. J., and Royer, C. A. (1998) Probing the contribution of internal cavities to the volume change of protein unfolding under pressure, *Protein Sci. 7*, 2217−2222.
37. Desai, G., Panick, G., Zein, M., Winter, R., and Royer, C. A. (1999) Pressure-jump studies of the folding/unfolding of trp repressor, *J. Mol. Biol. 288*, 461−475.
38. Jacob, M. H., Saudan, C., Holtermann, G., Martin, A., Perl, D., Merbach, A. E., and Schmid, F. X. (2002) Water contributes actively to the rapid crossing of a protein unfolding barrier, *J. Mol. Biol. 318*, 837−845.
39. Kitahara, R., Royer, C., Yamada, H., Boyer, M., Saldana, J. L., Akasaka, K., and Roumestand, C. (2002) Equilibrium and pressure-jump relaxation studies of the conformational transitions of P13MTCP1, *J. Mol. Biol. 320*, 609−628.
40. Mohana-Borges, R., Silva, J. L., Ruiz-Sanz, J., and de Prat-Gay, G. (1999) Folding of a pressure-denatured model protein, *Proc. Natl. Acad. Sci. U.S.A. 96*, 7888−7893.
41. Pappenberger, G., Saudan, C., Becker, M., Merbach, A. E., and Kiefhaber, T. (2000) Denaturant-induced movement of the transition state of protein folding revealed by high-pressure stopped-flow measurements, *Proc. Natl. Acad. Sci. U.S.A. 97*, 17−22.
42. Tan, C. Y., Xu, C. H., Wong, J., Shen, J. R., Sakuma, S., Yamamoto, Y., Lange, R., Balny, C., and Ruan, K. C. (2005) Pressure Equilibrium and Jump Study on Unfolding of 23-kDa Protein from Spinach Photosystem II, *Biophys. J. 88*, 1264−1275.
43. Baldisseri, D. M., Torchia, D. A., Poole, L. B., and Gerlt, J. A. (1991) Deletion of the ω-loop in the active site of staphylococcal nuclease. 2. Effects on protein structure and dynamics, *Biochemistry 30*, 3628−3633.
44. Chen, J., Lu, Z., Sakon, J., and Stites, W. E. (2000) Increasing the thermostability of staphylococcal nuclease: Implications for the origin of protein thermostability, *J. Mol. Biol. 303*, 125−130.
45. Dwyer, J. J., Gittis, A. G., Karp, D. A., Lattman, E. E., Spencer, D. S., Stites, W. E., and Garcia-Moreno, E. B. (2000) High apparent dielectric constants in the interior of a protein reflect water penetration, *Biophys. J. 79*, 1610−1620.
46. Fitch, C. A., Karp, D. A., Lee, K. K., Stites, W. E., Lattman, E. E., and Garcia-Moreno, E. B. (2002) Experimental pK_a values of buried residues: Analysis with continuum methods and role of water penetration, *Biophys. J. 82*, 3289−3304.
47. Garcia-Moreno, B., Dwyer, J. J., Gittis, A. G., Lattman, E. E., Spencer, D. S., and Stites, W. E. (1997) Experimental measurement of the effective dielectric in the hydrophobic core of a protein, *Biophys. Chem. 64*, 211−224.
48. Karp, D. A., Gittis, A. G., Stahley, M. A., Fitch, C. A., Stites, W. E., Lattman, E. E., and Garcia-Moreno, B. (2006) Molecular determinants of the abnormal pK_a value of an internal aspartic acid: Contributions by local unfolding and water penetration, submitted.
49. Nguyen, D. M., Leila, R. R., Gittis, A. G., and Lattman, E. E. (2004) X-ray and thermodynamic studies of staphylococcal nuclease variants I92E and I92K: Insights into polarity of the protein interior, *J. Mol. Biol. 341*, 565−574.
50. Stites, W. E., Gittis, A. G., Lattman, E. E., and Shortle, D. (1991) In a staphylococcal nuclease mutant the side-chain of a lysine replacing valine 66 is fully buried in the hydrophobic core, *J. Mol. Biol. 221*, 7−14.
51. Shortle, D., and Meeker, A. K. (1986) Mutant forms of staphylococcal nuclease with altered patterns of guanidine hydrochloride and urea denaturation, *Proteins 1*, 81−89.
52. Neuman, R. C., Jr., Kauzmann, W., and Zipp, A. (1973) Pressure dependence of weak acid ionization in aqueous buffers, *J. Phy. Chem. 77*, 2687−2691.
53. Royer, C. A., Hinck, A. P., Loh, S. N., Prehoda, K. E., Peng, X., Jonas, J., and Markley, J. L. (1993) Effects of amino acid substitutions on the pressure denaturation of staphylococcal nuclease as monitored by fluorescence and nuclear magnetic resonance spectroscopy, *Biochemistry 32*, 5222−5232.
54. Vidugiris, G. J., Truckses, D. M., Markley, J. L., and Royer, C. A. (1996) High-pressure denaturation of staphylococcal nuclease proline-to-glycine substitution mutants, *Biochemistry 35*, 3857−3864.
55. Denisov, V. P., Schlessman, J. L., Garcia-Moreno, E. B., and Halle, B. (2004) Stabilization of internal charges in a protein: Water penetration or conformational change? *Biophys. J. 87*, 3982−3994.
56. Damjanovic, A., Garcia-Moreno, B., Lattman, E. E., and Garcia, A. E. (2005) Molecular dynamics study of water penetration in staphylococcal nuclease, *Proteins 60*, 433−449.
57. Frye, K. J., and Royer, C. A. (1997) The kinetic basis for the stabilization of staphylococcal nuclease by xylose, *Protein Sci. 6*, 789−793.
58. Walkenhorst, W. F., Green, S. M., and Roder, H. (1997) Kinetic evidence for folding and unfolding intermediates in staphylococcal nuclease, *Biochemistry 36*, 5795−5805.
59. Hillson, N., Onuchic, J. N., and Garcia, A. E. (1999) Pressure-induced protein-folding/unfolding kinetics, *Proc. Natl. Acad. Sci. U.S.A. 96*, 14848−14853.
60. Bryngelson, J. D., Onuchic, J. N., Socci, N. D., and Wolynes, P. G. (1995) Funnels, pathways, and the energy landscape of protein folding: A synthesis, *Proteins 21*, 167−195.

61. Garcia, A. E., and Onuchic, J. N. (2003) Folding a protein in a computer: An atomic description of the folding/unfolding of protein A, *Proc. Natl. Acad. Sci. U.S.A. 100*, 13898−13903.
62. Hummer, G., Garde, S., Garcia, A. E., Paulaitis, M. E., and Pratt, L. R. (1998) The pressure dependence of hydrophobic interactions is consistent with the observed pressure denaturation of proteins, *Proc. Natl. Acad. Sci. U.S.A. 95*, 1552−1555.

BI052638Z